Maintenance of Proper Germline Stem Cell Number Requires Adipocyte Collagen in Adult *Drosophila* Females

Lesley N. Weaver and Daniela Drummond-Barbosa[1]
Department of Biochemistry and Molecular Biology, Bloomberg School of Public Health, Johns Hopkins University, Baltimore, Maryland 21205
ORCID IDs: 0000-0002-3120-8301 (L.N.W.); 0000-0002-7330-457X (D.D.-B.)

ABSTRACT Stem cells reside in specialized niches and are regulated by a variety of physiological inputs. Adipocytes influence whole-body physiology and stem cell lineages; however, the molecular mechanisms linking adipocytes to stem cells are poorly understood. Here, we report that collagen IV produced in adipocytes is transported to the ovary to maintain proper germline stem cell (GSC) number in adult *Drosophila* females. Adipocyte-derived collagen IV acts through β-integrin signaling to maintain normal levels of E-cadherin at the niche, thereby ensuring proper adhesion to GSCs. These findings demonstrate that extracellular matrix components produced in adipocytes can be transported to and incorporated into an established adult tissue to influence stem cell number.

KEYWORDS germline stem cells; adipocytes; collagen IV; oogenesis; *Drosophila*

TISSUE-RESIDENT stem cells within living organisms are constantly influenced by physiological factors (Ables *et al.* 2012). Adipocytes are required for energy homeostasis and secrete a variety of factors that can signal their physiological status to other tissues (Rosen and Spiegelman 2014). Adipocyte function is often disrupted in obese individuals, leading to an increased risk of metabolic diseases and cancers (Rosen and Spiegelman 2014). However, how adipocytes modulate tissue stem cells remains largely unknown.

The *Drosophila melanogaster* ovary is a powerful model to study the *in vivo* regulation of stem cells (Laws and Drummond-Barbosa 2017). Egg production in *Drosophila* is supported by self-renewing germline stem cells (GSCs). Each ovary contains 16–20 ovarioles comprising an anterior germarium followed by progressively older follicles (Figure 1A). The germarium houses two to three GSCs, which are supported by a somatic niche composed primarily of cap cells (Figure 1B). GSCs self-renew and give rise to a cystoblast that undergoes four rounds of synchronous divisions to generate a 16-cell germline cyst that will ultimately produce a mature oocyte (Laws and Drummond-Barbosa 2017). Cap cells promote GSC self-renewal by secreting Bone Morphogenic Protein (BMP) signals that prevent differentiation (Xie and Spradling 1998). E-cadherin-mediated adhesion of the niche to GSCs ensures their maintenance in the niche environment (Song and Xie 2002). Multiple systemic inputs, including unknown factors produced by adipocytes (Figure 1C), impinge on the local regulation of GSCs to functionally tie GSCs to the physiology of the organism as a whole (Laws and Drummond-Barbosa 2017; Matsuoka *et al.* 2017).

We previously took a proteomic approach to identify diet-regulated adult fat body factors with potential roles in the ovarian GSC lineage (Matsuoka *et al.* 2017). The fat body is a nutrient-sensitive organ composed of a majority of adipocytes in combination with smaller and fewer hepatocyte-like oenocytes (Arrese *et al.* 2010). We found that many extracellular matrix proteins, including collagen IV, rapidly accumulate in the fat body within 12 hr of a rich-to-poor diet shift (Matsuoka *et al.* 2017). Extracellular matrix proteins have structural and signaling roles, and type IV collagens are particularly abundant in basement membranes (Brizzi *et al.* 2012). In *Drosophila*, collagen IV is encoded by *Collagen type IV α 1* (*Col4α1*, also known as *Cg25C*) and *Viking*, and previous work showed that the larval fat body produces

doi: https://doi.org/10.1534/genetics.118.301137
Manuscript received April 18, 2018; accepted for publication May 31, 2018; published Early Online June 8, 2018.
Supplemental material available at Figshare: https://doi.org/10.25386/genetics.6463229.
[1]Corresponding author: Department of Biochemistry and Molecular Biology, Bloomberg School of Public Health, Johns Hopkins University, 615 N. Wolfe St., Room W3118, Baltimore, MD 21205. E-mail: dbarbosa@jhu.edu

heterotrimers of Viking and Cg25C that are transported through the hemolymph and deposited in developing organs (Pastor-Pareja and Xu 2011). By contrast, the source and role of collagen IV in the adult, fully established ovary remains largely unexplored.

In this study, we used a combination of genetics and cell biology to investigate whether and how adipocyte-derived collagen IV modulates the *Drosophila* female GSC lineage. We demonstrate that collagen IV produced in adipocytes is transported to and incorporated into the established GSC niche region to support GSC maintenance in adult females. We show that, while cap cell number and BMP signaling remain intact, adipocyte-specific knockdown of collagen IV reduces E-cadherin levels in the niche. Further, we find that focal adhesion kinase (FAK) is required in the niche to regulate E-cadherin levels and GSC number, and that adipocyte collagen IV regulates GSC maintenance through a genetic interaction with β-integrin and FAK. Taken together, our results show that extracellular matrix proteins secreted from adult adipocytes can influence stem cell behavior in a distinct, fully established tissue.

Materials and Methods

Drosophila strains and culture conditions

Drosophila stocks were maintained at 22–25° on standard medium containing cornmeal, molasses, agar, and yeast. Standard medium supplemented with wet yeast paste was used for all experiments, except where noted. Previously described Gal4 lines were used, including *3.1Lsp2-Gal4* (Armstrong *et al.* 2014), *bab1-Gal4* (Cabrera *et al.* 2002), *MTD-Gal4* (Ni *et al.* 2011), and *Cg-Gal4* (Asha *et al.* 2003). The temperature-sensitive *tub-Gal80^{ts}* transgene and the *dad::nlsGFP* reporter have been described (McGuire *et al.* 2003; Ayyaz *et al.* 2015). The *Fak^{KG00304}* (Tsai *et al.* 2008), *vkg^{01209}* (Spradling *et al.* 1999), *Cg25C^{K00405}* (Spradling *et al.* 1999), *scb^{2}* (Stark *et al.* 1997), *shg^{2}* (Tepass and Hartenstein 1994), and *dpp^{e87}* (Wharton *et al.* 1993) alleles were obtained from the Bloomington *Drosophila* Stock Center (BDSC, bdsc.indiana.edu/). The *vkg^{KG07138}* allele (Rodriguez *et al.* 1996) was obtained from the Kyoto Stock Center (www.dgrc.kit.ac.jp/). The GFP protein trap line *Vkg^{G00454}* (Pastor-Pareja and Xu 2011) was a generous gift from Bill Chia. The *UAS-GFP hairpin* line was previously described (Pastor-Pareja and Xu 2011). *UAS-luc^{JF01355}* (Matsuoka *et al.* 2017), *UAS-vkg^{HMC02910}* (Ni *et al.* 2011), *UAS-SPARC^{HMS02133}* (Ni *et al.* 2011), *UAS-Fak^{HMS00010}* (Ni *et al.* 2011), and *UAS-Fak^{HMS02792}* (Ni *et al.* 2011) Transgenic RNAi (RNA interference) Project (fgr.hms.harvard.edu/) lines were obtained from the BDSC. Additional *UAS-hairpin* lines were obtained from the Vienna *Drosophila* RNAi stock Center (VDRC, stockcenter.vdrc.at/), including *UAS-vkg^{GD5246}* (Pastor-Pareja and Xu 2011), *UAS-Cg25C^{GD12784}* (Neely *et al.* 2010), *UAS-Cg25C^{KK104536}* (Langer *et al.* 2010), and *UAS-SPARC^{GD5660}* (Neely *et al.* 2010). Lines carrying multiple genetic elements were generated by standard crosses. Balancer chromosomes, *FRT* and *FLP* strains, and other genetic elements are described in FlyBase (www.flybase.com).

Tissue- and cell type-specific RNAi

Females of genotypes *y w; tub-Gal80^{ts}/UAS-hairpin; 3.1Lsp2-Gal4/+* or *y w; tub-Gal80^{ts}/+; 3.1Lsp2-Gal4/UAS-hairpin* (for adult adipocyte-specific RNAi), and *y w; tub-Gal80^{ts}/UAS-hairpin; bab1-Gal4/+* or *y w; tub-Gal80^{ts}/+; bab1-Gal4/UAS-hairpin* (for adult-specific niche RNAi), were raised at 18° [the permissive temperature for Gal80^{ts} (McGuire *et al.* 2003)] to prevent RNAi induction during development. Zero- to 2-day-old females were maintained at 18° for 3 days with *y w* males, and then switched to 29° (the restrictive temperature for Gal80^{ts}) for various lengths of time to induce RNAi in specific adult tissues (*UAS-luc^{JF01355}* was used as an RNAi control). To control for leaky upstream activating sequence (UAS) expression, females of similar genotypes but without *Gal4* and *Gal80^{ts}* transgenes were raised and maintained under the same conditions for analysis at 12 days after switch to 29°. MTD-Gal4 experiments were performed as described above, except that Gal80^{ts} was not included and females were raised at 25° instead of 18° before shifting to 29°.

Genetic mosaic analysis

Females of genotype *y w hs-FLP*; *ubi-GFP FRT40A/vkg* FRT40A* or *y w hs-FLP*; *ubi-GFP FRT40A/Cg25C* FRT40A* were generated through standard crosses (*vkg** and *Cg25C** represent null or wild-type alleles of the respective genes). Zero- to 3-day-old females were maintained on standard food with dry yeast and heat-shocked twice daily at 37° for 3 days to induce flipase (FLP)/*FLP recognition target* (*FRT*)-mediated mitotic recombination, as described (LaFever and Drummond-Barbosa 2005; Hsu *et al.* 2008; Hsu and Drummond-Barbosa 2009, 2011; Ables and Drummond-Barbosa 2010, 2013; LaFever *et al.* 2010; Ables *et al.* 2015, 2016; Laws and Drummond-Barbosa 2015, 2016; Laws *et al.* 2015). After the final heat shock, females were kept on standard medium supplemented with wet yeast paste for 10 days prior to dissection. *vkg** and *Cg25C** homozygous clones were recognized by the absence of GFP, and GSCs were identified based on their anterior location and typical fusome morphology (Laws and Drummond-Barbosa 2015). To quantify GSC loss, germaria containing GFP-negative cystoblasts and/or cysts were analyzed, and the percentage of germaria that no longer contained the GFP-negative GSC that gave rise to those GFP-negative progeny (*i.e.*, "GSC loss events") was calculated (Laws and Drummond-Barbosa 2015). At least three independent experiments were performed and statistical significance was calculated using the Student's *t*-test.

Ovary and fat body immunostaining and fluorescence microscopy

Ovaries were dissected in Grace's Insect Medium (Bio Whittaker) and, after teasing ovarioles apart, fixed for 13 min in 5.3% formaldehyde (Ted Pella) in Grace's medium at room

temperature. Ovaries were subsequently rinsed once and washed three times for 15 min in PBT (PBS: 10 mM NaH_2PO_4/$NaHPO_4$ and 175 mM NaCl, pH 7.4, plus 0.1% Triton X-100). Samples were blocked for 3 hr in 5% normal goat serum (NGS; Jackson ImmunoResearch) plus 5% bovine serum albumin (BSA; Sigma [Sigma Chemical], St. Louis, MO) in PBT, and then incubated overnight at 4° in the following primary antibodies diluted in blocking solution: mouse monoclonal anti-α-Spectrin (3A9) [1:25; DSHB (Developmental Studies Hybridoma Bank)]; mouse anti-Lamin C (LC28.26) (1:100; DSHB); chicken anti-GFP (1:1000; Abcam); rat monoclonal anti-E-cadherin (DCAD2) (1:3; DSHB); and rabbit anti-pFAK (Y397) (1:100; Invitrogen, Carlsbad, CA). Samples were washed in PBT and incubated for 2 hr at room temperature in 1:400 Alexa Fluor 488- or 568-conjugated goat species-specific secondary antibodies (Molecular Probes, Eugene, OR). Samples were washed and ovaries were mounted in Vectashield containing 1.5 μg/ml 4',6-diamidino-2-phenylindole (DAPI) (Vector Laboratories, Burlingame, CA). Images were collected with Zeiss (Carl Zeiss, Thornwood, NY) AxioImager-A2 fluorescence or LSM700 confocal microscopes.

Abdominal carcasses with the fat body attached (but without guts and ovaries) were fixed as above, except for 20 min instead of 13 min. Fat bodies attached to carcasses were washed as above, incubated with Alexa Fluor 488-conjugated phalloidin (1:200; Molecular Probes) in PBT for 20 min, rinsed, and washed three times for 15 min in PBT. Alternatively, fat bodies were stained with DCAD2 as described above. For Vkg::GFP analysis, fat bodies were stained with chicken anti-GFP as described above. Samples were stored in Vectashield plus DAPI (Vector Laboratories) containing 25 ng/ml Nile Red dye, and fat bodies were scraped off the abdominal carcass before mounting and imaging on a Zeiss LSM700 confocal microscope.

For Dad::nlsGFP quantification, the densitometric mean of individual GSC nuclei was measured from optical sections containing the largest nuclear diameter (visualized by DAPI) using ImageJ (Armstrong *et al.* 2014). For E-cadherin quantification, the total densitometric value from maximum intensity projections around the cap cells (identified by LamC staining) were measured with ImageJ. Quantification of E-cadherin levels by immunofluorescence is a well-established method to determine whether adherence of GSCs to the niche is compromised (Hsu and Drummond-Barbosa 2011; Ables and Drummond-Barbosa 2013; Tseng *et al.* 2014; Laws *et al.* 2015; Lee *et al.* 2016). Densitometric data were subjected to the Mann–Whitney *U*-test. To measure adipocyte nuclear diameter, the largest nuclear diameter of each adipocyte (visualized by DAPI) was measured using ImageJ. To measure adipocyte area, the largest cell area of each adipocyte (based on phalloidin or DCAD2 staining) was measured using ImageJ. Data were subjected to the Student's *t*-test.

Quantification of cap cells, GSCs, and GSC progeny

Cap cells were identified based on their ovoid shape and strong Lamin C staining, whereas GSCs were identified based on their juxtaposition to cap cells and typical fusome morphology, as described (Laws and Drummond-Barbosa 2015). Two-way ANOVA with interaction (GraphPad Prism) was used to calculate the statistical significance of any differences among genotypes in how much cap cell or GSC numbers change over time (*e.g.*, rate of GSC loss) from at least three independent experiments. In accordance with our choice to use two-way ANOVA with interaction analysis, we had independent observations, our data did not display any significant outliers, our dependent variable was normally distributed for each independent variable, and there was equal variance for each independent variable group. The dependent variables determined for two-way ANOVA with interaction were either GSC or cap cell number, whereas the two independent variables were genotype and time (Armstrong *et al.* 2014). Cystoblasts and 2-, 4-, 8-, and 16-cell germline cysts present in germaria were identified based on fusome morphology, and the number of GSC progeny in each stage was normalized to the number of GSCs in all the germaria analyzed (Laws and Drummond-Barbosa 2015). The average number of cystoblasts and cysts per GSC was calculated from at least three independent experiments and subjected to the Student's *t*-test.

Quantification of Vkg::GFP transport from adipocytes to the GSC region

To determine whether Vkg is transported from adult adipocytes to the ovary, we designed an *in vivo* experiment that would allow us to "track" Vkg::GFP fluorescence originating from adipocytes over time. We generated females that contained one copy of *vkg*::*GFP*, which is endogenously tagged and fully functional (Pastor-Pareja and Xu 2011), and one copy of wild-type *vkg* in combination with the adipocyte-specific *tub-Gal80^{ts};3.1Lsp2-Gal4* (*3.1Lsp2^{ts}*) (Armstrong *et al.* 2014) driver and a *UAS-GFP hairpin* transgene (the presence of the untagged *vkg* allele ensures that knockdown of *vkg*::*GFP* using *GFP* RNAi will leave mRNA from one of the *vkg* alleles unaffected at all times, precluding any confounding phenotypes). To knock down *vkg*::*GFP* specifically in adipocytes during development, females were raised at 29° (to inactivate *Gal80^{ts}* and allow *GFP hairpin* expression). Newly eclosed females were either dissected immediately ($t = 0$), maintained in triplicate vials with *y w* males at 29° for 21 days (to keep Vkg::GFP off in adult adipocytes), or shifted to 18° for 21 days (to allow Vkg::GFP expression in adult adipocytes) prior to dissection and analysis of their fat bodies and ovaries.

To measure Vkg::GFP fluorescence intensity in adipocytes, the maximum intensity of each of five evenly spaced lines intersecting the basement membrane of a field of adipocytes was measured and averaged. Twenty or more randomly selected fields of adipocytes from three independent experiments were analyzed. As a measure of *GFP* RNAi efficiency, adipocyte Vkg::GFP fluorescence intensity at $t = 0$ was measured and compared to adipocyte samples from 21 days at 29° *vs.* 18°. The increase in Vkg::GFP fluorescence intensity in adipocytes from 21 days at 18° indicated that our experimental set up was working as expected to knockdown and restore

adipocyte-specific Vkg::GFP levels. As an additional control, we measured the levels of Vkg::GFP in stage 6–8 follicles as described above for adipocytes. In agreement with the known local production of collagen IV in these follicles (Haigo and Bilder 2011), the levels of Vkg::GFP surrounding them were unaffected by Vkg::GFP manipulations in adipocytes. To quantify Vkg::GFP intensity in the GSC region, five independent maximum intensity line measurements (as above) were obtained in the anterior portion of the germarium (*i.e.*, the basement membrane adjacent to cap cells) and averaged. Twenty or more germaria from three independent experiments were analyzed. To achieve as much consistency as possible among samples for intensity measurements, samples were dissected, fixed, and stained in parallel under identical conditions, and the image acquisition settings were exactly the same for all images used for quantification. All measurements were recorded using ImageJ for at least three independent experiments. Data were subjected to the Mann–Whitney *U*-test.

Reverse transcriptase-polymerase chain reaction

For RNA extraction, five whole females were incubated in RNAlater (Ambion) for 30 min according to the manufacturer's instructions to stabilize RNA. Alternatively, carcasses (*i.e.*, females without their ovaries and gut) from 20 females or ovaries from five females per genotype were hand dissected in RNAlater and incubated on ice for 30 min. Fat bodies were then scraped off the cuticle in a dissecting well containing 250 μl lysis buffer from the RNAqueous-4PCR DNA-free RNA Isolation for RT-PCR kit (Ambion), whereas 250 μl of lysis buffer was added to ovary and whole-female samples. RNA was extracted from all samples using a motorized pestle and following the manufacturer's directions. cDNA was synthesized using the SSRII kit (Ambion) according to the manufacturer's instructions. The primers used for PCR reactions are listed in Supplemental Material, Table S1. *Rp49* primers were used as a control. Net band intensity for each sample was quantified using ImageJ by subtracting background pixels from band pixels in a fixed size box, and normalized to the net band intensity of the corresponding *Rp49* band. Controls were set to one and experimental sample intensities were calculated relative to control.

Data availability

Drosophila strains are available upon request. All data generated for this study are included in the main text and figures or in the supplemental files provided. Supplemental material available at Figshare: https://doi.org/10.25386/genetics.6463229.

Results

Adipocyte-derived collagen IV is specifically required for GSC maintenance

In the adult female fat body, collagen IV proteins are abundant and highly regulated (Matsuoka *et al.* 2017), leading us to ask whether collagen IV in adipocytes might be connected to the maintenance of GSCs. We knocked down *viking* (*vkg*), *Cg25C* (both of which encode collagen IV), or SPARC (which encodes a collagen-binding protein) specifically in adult adipocytes using the previously described *tub-Gal80^{ts}*; *3.1Lsp2-Gal4* (*3.1Lsp2^{ts}*) driver (Armstrong *et al.* 2014) to induce *UAS-hairpin* transgenes for RNAi. Adult adipocyte-specific *vkg*, *Cg25C*, or *SPARC* RNAi significantly increased the rate of GSC loss (Figure 1, D–G and Figure S1). There were no changes in cap cell number (Figure S1), germline development or survival (Figure S2, A–C), or adipocyte morphology (Figure S2, D–F), underscoring the specificity of the effect of adipocyte collagen IV knockdown on GSCs.

Collagen IV is not required cell-autonomously for GSC maintenance

We next wondered how collagen IV produced in adipocytes might influence GSC number in the ovary. However, as a first step we examined whether more locally produced collagen IV also affects GSC maintenance. Collagens are typically transcribed and secreted locally, and collagen IV represents the major structural component of basement membranes (Frantz *et al.* 2010). In the adult *Drosophila* ovary, collagen IV surrounds the germarium (including the GSC niche region) and developing follicles (Haigo and Bilder 2011), as can be readily visualized using a fully functional, endogenously tagged Vkg::GFP protein fusion (Haigo and Bilder 2011; Pastor-Pareja and Xu 2011) (Figure S3, A and B). By contrast, a Gal4 transgene under the control of the 2.7-kb regulatory region shared by *Cg25C* and *vkg* (Asha *et al.* 2003; Zabidi and Stark 2016) (Figure S3A), while sufficient to drive *UAS-nuclear GFP* expression in follicle cells of later follicles [which are known to produce their own collagen (Haigo and Bilder 2011)], showed no detectable activity in the early stages of oogenesis, including the germarium (Figure S3C). Given that transcription of collagen IV might still occur despite not being detectable by this Gal4 reporter, we genetically addressed whether collagen IV from the germline or niche is functionally relevant. Genetic mosaic analysis using *Cg25C* and *vkg* null alleles did not reveal any cell-autonomous role of collagen IV in the regulation of GSC number in adult females (Figure S3, D–F). Given that genetic mosaic analysis is not feasible in the adult GSC niche, we instead used *tub-Gal80^{ts}*; *bab1-Gal4* to induce collagen IV RNAi specifically in the adult niche (akin to the adult adipocyte knockdown approach above). Knockdown of *vkg* in the niche using the stronger (but not the weaker) RNAi line led to a slight increase in GSC loss (Figure S3, G and H). These results indicate that adipocytes are the major site of collagen IV requirement for GSC maintenance, with a smaller contribution from the niche. Further, they suggest that it is unlikely that local transcription of collagen IV accounts for all the collagen IV protein maintained around the niche and early stages of oogenesis.

Adipocyte-derived collagen IV is incorporated into the adult ovary basement membrane

We next investigated adipocytes as a possible cellular source of collagen IV in the GSC niche region in adult females. During

Drosophila development, collagen IV is produced by hemocytes and deposited around the developing GSC niche, where it limits BMP signaling and the number of initial GSCs established (Pastor-Pareja and Xu 2011; Van De Bor *et al.* 2015). The developing fat body also produces and secretes collagen IV, which is deposited into the extracellular matrix of other developing organs (Pastor-Pareja and Xu 2011). To directly test whether collagen IV is transported from adipocytes to the fully established GSC niche in adult females, we took advantage of the Vkg::GFP endogenous fusion (Figure S3, A and B) and our ability to target it for degradation specifically in adipocytes using the *3.1Lsp2^{ts}* driver and a *UAS-GFP hairpin* transgene (Figure 2). In females carrying a wild-type untagged *vkg* allele *in trans* to the tagged *vkg*::*GFP* allele at 29° (where Gal80^{ts} is inactive), *3.1Lsp2^{ts}* induces *GFP* RNAi and thus knockdown of *vkg*::*GFP* in adipocytes only, leaving expression of the untagged Vkg intact. At 18° (where Gal80^{ts} is active), *3.1Lsp2^{ts}* is off and Vkg::GFP can be expressed in adipocytes. Females were raised at 29° to inhibit expression of Vkg::GFP from adipocytes during development (Figure 2A). As expected, we detected very low levels of Vkg::GFP in adipocytes of newly eclosed females (Figure 2, B and C, left panels). Vkg::GFP levels were also low in the GSC region (Figure 2, D and E, left panels). A subset of newly eclosed females was maintained at 29° for 21 days to continuously knock down adipocyte Vkg::GFP, whereas another subset was maintained at 18° to allow Vkg::GFP expression in adult adipocytes (Figure 2A). Remarkably, if Vkg::GFP remained repressed in adult adipocytes (29°) (Figure 2, B and C, middle panels), the GSC region maintained low levels of Vkg::GFP (Figure 2, D and E, middle panels), whereas if Vkg::GFP expression in adult adipocytes was allowed (18°) (Figure 2, B and C, right panels), there was a significant increase in Vkg::GFP intensity in the GSC region (Figure 2, D and E, right panels). By contrast, the levels of Vkg::GFP surrounding older developing follicles (stages 6–8) were unaffected by the status of Vkg::GFP expression in adult adipocytes (Figure 2, F and G), consistent with the local production of collagen IV in these later stages (Haigo and Bilder 2011). Taken together, these results indicate that adipocytes are a major source of newly deposited collagen IV for the established GSC region of adult females, although they do not rule out contributions from other conceivable remote sources of collagen IV.

Adipocyte collagen IV does not influence BMP signaling, but is required for maintaining normal E-cadherin levels in the GSC niche

Our finding that collagen IV is transported from adipocytes to the GSC region suggested effects on BMP signaling or E-cadherin as possible mechanisms for how adipocyte-derived collagen IV might affect GSC number. To determine whether adipocyte collagen IV influences BMP signaling, we measured the nuclear intensity of the BMP signaling reporter Dad::nlsGFP in GSCs when *vkg* was knocked down in adult adipocytes. *vkg* RNAi in adult adipocytes did not change Dad::nlsGFP levels in GSC nuclei compared to control RNAi (Figure 3, A and B). By contrast, *vkg* knockdown in adult adipocytes significantly decreased the total levels of E-cadherin in cap cells relative to controls (Figure 3, C and D), suggesting that GSCs are lost due to reduced adhesion to the niche.

FAK is required in the niche for GSC maintenance

We next explored the molecular connection between adipocyte-derived collagen IV and E-cadherin regulation in the niche. In mammalian cells, collagen IV stimulation of integrins and downstream activation of FAK signaling leads to down-regulation of E-cadherin (Canel *et al.* 2013). Type IV collagen-induced activation of FAK is associated with an epithelial-to-mesenchymal transition-like process in mammary epithelial cells (Espinosa Neira and Salazar 2012). Conversely, another study showed that a specific region of collagen IV promotes cell adhesion in several cancer cell lines (Miles *et al.* 1994). As a first step, we asked if cap cells or GSCs might require FAK signaling to maintain E-cadherin levels and normal GSC numbers. We knocked down *Fak* specifically in the germline or in the adult niche using the *MTD-Gal4* or *tub-Gal80^{ts}*; *bab1-Gal4* (*bab1^{ts}*) drivers, respectively, and available *UAS-hairpin* transgenes (Figure 3, E–H and Figure S4, A–E). Knockdown of *Fak* in the germline slightly decreased GSC number (Figure S4, C–E), whereas adult niche *Fak* knockdown led to a significant increase in GSC loss rates (Figure 3, E and F and Figure S4, A and B). In addition, *Fak* RNAi in the niche caused a reduction in the E-cadherin levels in cap cells (Figure 3, G and H), similar to what we observed upon *vkg* RNAi in adipocytes (Figure 3, C and D). These results revealed that FAK signaling in the niche is required for proper E-cadherin levels and for GSC maintenance.

Collagen IV genetically interacts with integrin/FAK to regulate GSC maintenance

We then sought to test whether adipocyte collagen IV might affect GSC maintenance via integrin/FAK signaling-mediated control of E-cadherin levels. To directly test if collagen IV affects FAK signaling in the niche, we pursued a commercially available antibody specific for phosphorylated FAK, pFAK (Y395) (Fried *et al.* 2012). This phosphospecific antibody recognizes ring canals (which contain pFAK) within ovarian follicles (Figure S4G), as previously described (Dodson *et al.* 1998); however, we were unable to detect specific signals in the GSC niche regions (Figure S4F), precluding our intended experiment. This is simply a technical limitation (as opposed to reflecting a lack of FAK activity in the niche), given the clear genetic requirement for *Fak* in niche cells (see Figure 3, E and F). We next examined genetic interactions between collagen IV, integrin signaling components, and E-cadherin. First, we reasoned that if adipocyte-derived Vkg acts through FAK to control E-cadherin levels and GSC maintenance, decreasing the levels of FAK might enhance the GSC loss phenotype of adipocyte *vkg* RNAi. Therefore, we knocked down *vkg* specifically in adipocytes of adult females heterozygous for the hypomorphic *Fak^{KG00304}* allele (Figure 4A). GSC maintenance was unaffected by the presence of one copy of

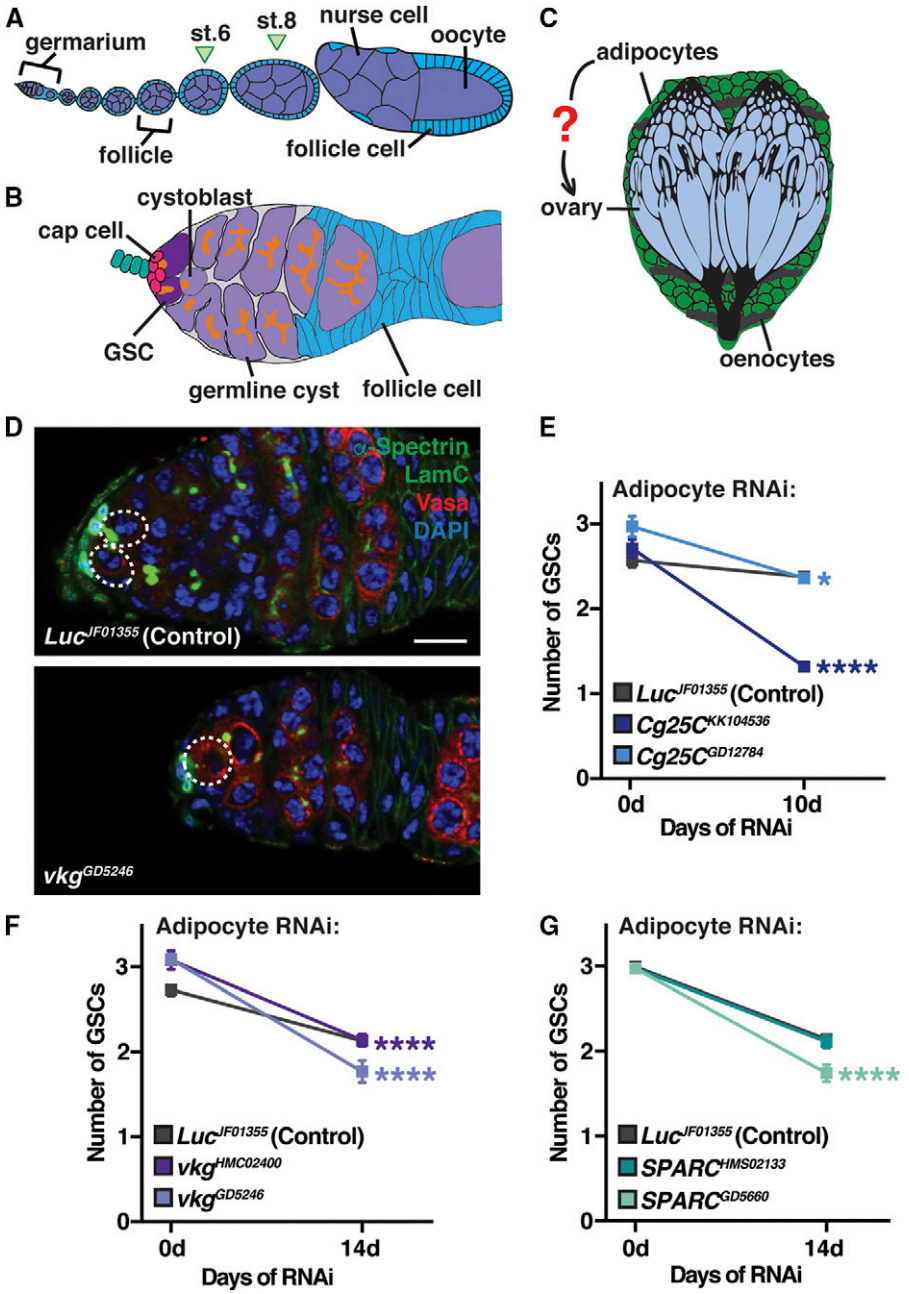

Figure 1 Collagen IV produced in adult adipocytes is required for GSC maintenance. (A) The *Drosophila* ovary is composed of 16–20 ovarioles that contain progressively older follicles. Each follicle consists of a germline cyst (one oocyte and 15 nurse cells) surrounded by somatic follicle cells (blue), and they are produced in the germarium at the anterior tip of each ovariole. (B) Each germarium contains two–three GSCs that reside in a somatic niche composed primarily of cap cells. GSCs divide asymmetrically to self-renew and generate a cystoblast that forms a 16-cell cyst. GSCs and germline cysts are identified based on the morphology and position of the fusome, a germline-specific organelle (de Cuevas and Spradling 1998). Follicle cells envelop the germline cyst to form a follicle. (C) The adult fat body (composed of adipocytes and hepatocyte-like oenocytes) surrounds the ovary. (D) Germaria at 14 days of adult adipocyte-specific *Luc* RNAi control or *vkg* RNAi. Vasa (red), germ cells; α-Spectrin (green), fusome; LamC (green), cap cell nuclear lamina; DAPI (blue), nuclei. GSCs are outlined. Bar, 10 μm. (E–G) Average number of GSCs per germarium over time of control, *Cg25C RNAi* (E), *vkg RNAi* (F), or *SPARC RNAi* (G) (mean ± SEM, * $P < 0.05$ and **** $P < 0.0001$, two-way ANOVA with interaction). See also Figures S1 and S2. GSC, germline stem cell; RNAi, RNA interference; st., stage.

$Fak^{KG00304}$ in control RNAi females [Figure 4B, compare control and experimental slopes (*i.e.*, rates of GSC loss) and see *Materials and Methods* for detailed explanation of statistical analysis]. By contrast, the rate of GSC loss of adipocyte *vkg* RNAi females was slightly but significantly increased by one copy of $Fak^{KG00304}$ (*i.e.*, in a dominant fashion), despite it not being a null allele (Figure 4B, compare control and experimental slopes). This dominant genetic interaction suggests that adipocyte-derived collagen IV and FAK work in a common pathway to maintain GSCs. We also carried out additional stringent genetic interaction tests using double heterozygous combinations of null alleles of *vkg* and *scab* (*scb*, which encodes α-PS3 integrin) or *shotgun* (*shg*, which encodes E-cadherin), using a null allele of *decapentaplegic* (*dpp*, which encodes a BMP signal) as a negative control. dpp^{e87} +/+ vkg^{01209} double heterozygotes had similar rates of GSC loss as single heterozygotes (Figure 4C), consistent with the observation that adipocyte collagen IV does not affect BMP signaling (Figure 3, A and B). Conversely, vkg^{01209} +/+ scb^2 and vkg^{01209} +/+ shg^2 double heterozygotes showed a small but significant increase in the rate of GSC loss compared to single heterozygous controls (Figure 4D). Collectively, our dominant genetic interaction results provide genetic evidence in support of the model that in adult females, adipocyte collagen IV functions through integrin/FAK signaling to regulate E-cadherin levels and GSC number.

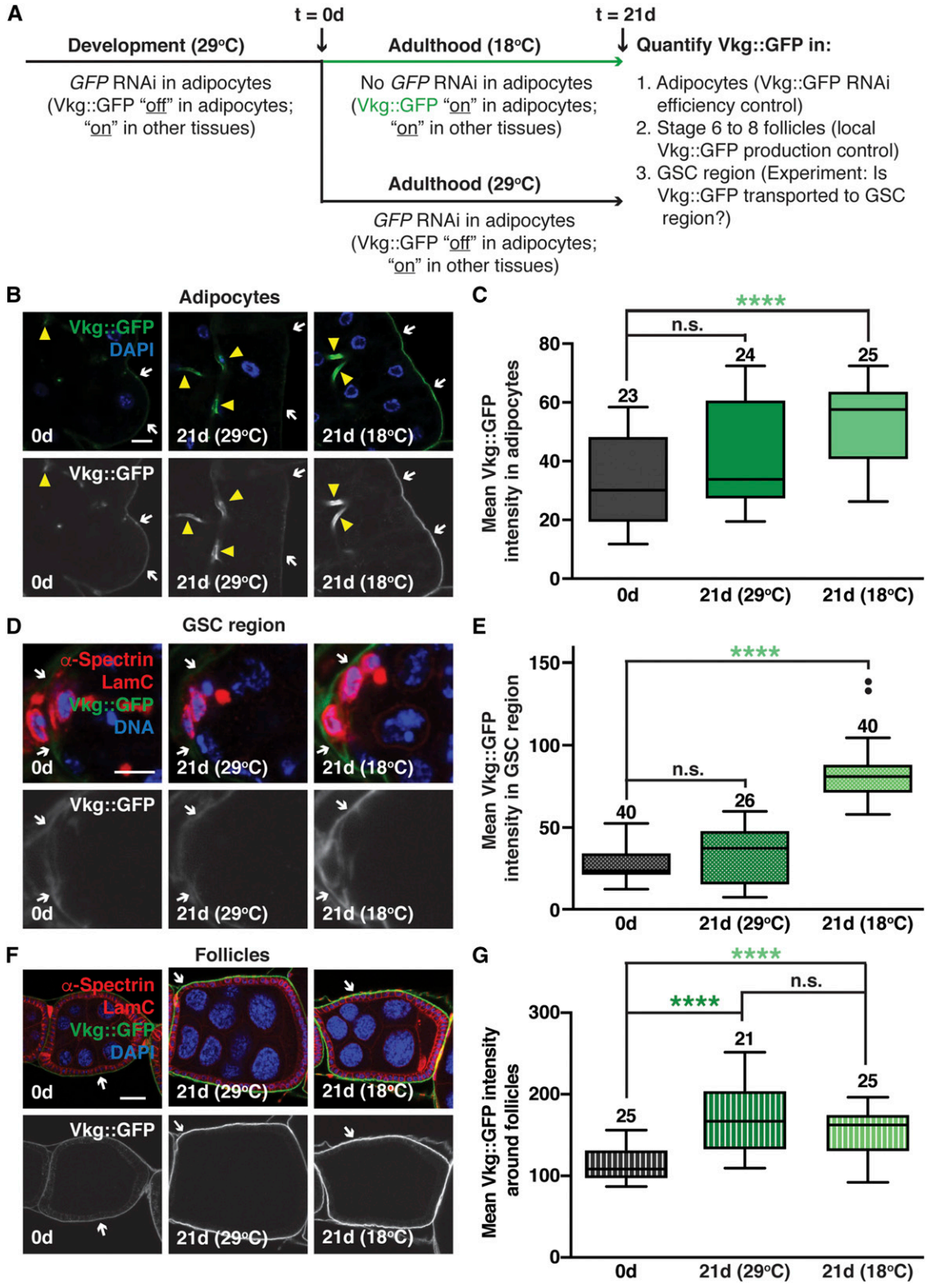

Figure 2 Collagen IV is transported from adipocytes to the GSC region in adult females. (A) Experimental design for adipocyte-specific *GFP* RNAi and analysis of Vkg::GFP distribution. Vkg::GFP was knocked down specifically during development using the *3.1Lsp2-Gal4* driver and a previously described *UAS-GFP shRNA*. After eclosion, females were immediately dissected, maintained at 29° (to maintain *GFP* RNAi), or switched to 18° (*GFP* RNAi off). After 21 days, females at 29 or 18° were dissected and analyzed for GFP fluorescence intensity. (B) Adipocytes from newly eclosed females (0d) and 21-day old (21d) females maintained at 29 or 18° showing higher levels of Vkg::GFP (arrows) at 18° (when adipocyte-specific *GFP* RNAi is off). GFP (green), Vkg::GFP; DAPI (blue), nuclei. Vkg::GFP shown in grayscale in bottom panels. Arrowheads indicate trachea. Bar, 10 μm. (C) Box-and-whisker plot of mean Vkg::GFP intensity in adipocytes for experiment shown in (B). (D) Germaria from females as in (B) showing that higher levels of Vkg::GFP in the

Discussion

Our data show that collagen IV is produced in adipocytes and transported to the ovary to influence the maintenance of GSCs in adult *Drosophila* females. To our knowledge, this is the first example of an extracellular matrix component produced in adipocytes being incorporated into a stem cell niche in a distinct, fully established adult tissue to regulate stem cell activity. Further, we also provide genetic evidence consistent with the model that collagen IV directly stimulates integrin/FAK signaling in the niche to maintain E-cadherin levels and thereby promote GSC maintenance. These results are widely relevant, considering the well-established link between obesity and a large number of cancers and other diseases (Rosen and Spiegelman 2014), and the diverse structural and signaling roles of collagen IV and other extracellular matrix components in development, tissue integrity and function, tumor biology, and aging (Frantz *et al.* 2010; Mao *et al.* 2015).

Differential effects of collagen IV on GSC numbers during development and adulthood

Here, our results show that adipocyte-derived collagen IV is required for GSC maintenance in adult ovaries. In contrast to these findings in adults, loss of collagen IV function during larval stages, either in hypomorphic alleles or by knocking down collagen IV in hemocytes, results in excess GSC-like cells that are readily apparent in newly eclosed females (Wang *et al.* 2008; Van De Bor *et al.* 2015). Cg25C and Viking can bind directly to Dpp, suggesting that this marked increase in GSC-like cell number reflects a role of collagen IV in limiting BMP signaling to GSCs during niche development (Wang *et al.* 2008). Conversely, we find that knockdown of adipocyte collagen IV in adults does not influence BMP signaling in the niche, instead promoting GSC maintenance via E-cadherin. These contrasting findings suggest that collagen IV has context-dependent roles in the regulation of GSC number, depending on whether or not the niche is fully established. However, this study does not rule out the possibility that collagen IV from additional adult tissues might also contribute to the GSC niche, potentially affecting BMP signaling.

Continuous remodeling of the adult GSC niche extracellular matrix

The extracellular matrix components support tissue integrity and homeostasis, and can also act as ligands for cell surface receptors to modify cell behavior (Brizzi *et al.* 2012). Collagen IV is produced and secreted from adipocytes to be incorporated into the basement membranes of developing tissues (Pastor-Pareja and Xu 2011), and hemocytes also produce collagen IV that is deposited in the ovary during development (Van De Bor *et al.* 2015; Matsubayashi *et al.* 2017). Yet, although newly eclosed females display a robust extracellular matrix in the GSC region, it is clear from our work that the fully established GSC region requires the deposition of new collagen IV derived from adipocytes during adulthood for proper maintenance of GSCs. These findings indicate an active role of extracellular matrix components in maintaining stem cell function during adulthood. Nevertheless, it remains unknown whether this process operates in a steady-state manner or is actively modulated under different physiological conditions to help control GSC number over time.

Collagen IV interacts with integrins to regulate cell–cell adhesion in various contexts

Our data suggest that adult adipocyte collagen IV interacts with integrins on the surface of niche cells to influence E-cadherin levels through FAK signaling. Indeed, collagen IV acts as a ligand for integrins, influencing cell adhesion, proliferation, and differentiation in mammalian epithelial and tissue culture models (Bonnans *et al.* 2014). Although the activation of integrin signaling elicits a wealth of signaling cascades (Harburger and Calderwood 2009), FAK is a known downstream effector of integrin signaling and regulator of adhesion (Legate *et al.* 2009). Depending on the context, FAK-mediated signaling can either increase or decrease cadherin levels. For example, FAK recruitment and activation at focal adhesions in motile HeLa cells downregulates Rac1 activity, reducing the levels of N-cadherin (Yano *et al.* 2004). Conversely, in mouse embryonic fibroblasts, FAK acts as a core component of focal adhesion signaling that activates Rac, resulting in increased expression of N-cadherin and adhesion (Mui *et al.* 2016). In addition, FAK activation is required in human colon carcinoma Moser cells to induce E-cadherin production (Wang *et al.* 2004). These results suggest that cell-to-cell adhesion and cell-to-extracellular matrix interactions can be antagonistic, cooperative, or possibly independent. Our findings that FAK is required in the niche to promote E-cadherin levels and GSC maintenance, and genetically interacts with integrin and Collagen IV to regulate these processes, add an *in vivo* and physiologically relevant example to this growing body of literature.

Remaining questions

Our results highlight collagen IV as an adipocyte-secreted factor required for GSC maintenance, raising several questions. For example, it is currently unknown what pathways are

GSC niche region result specifically from Vkg::GFP expression in adult adipocytes. GFP (green), Vkg::GFP; α-Spectrin (red), fusome; LamC (red), cap cell nuclear lamina; DAPI (blue), nuclei. Bar, 5 μm. (E) Box-and-whisker plot of mean Vkg::GFP intensity in the GSC region for experiment shown in (D). (F) Representative images of stage 6–8 egg chambers from females showing that levels of Vkg::GFP in developing egg chambers do not depend on Vkg::GFP expression in adult adipocytes. Bar, 25 μm. (G) Box-and-whisker plot of mean Vkg::GFP intensity for experiment in (F). **** $P < 0.0001$, Mann–Whitney *U*-test. Sample sizes are included above. See also Figure S3. GSC, germline stem cell; n.s., not significant; RNAi, RNA interference; shRNA, short hairpin RNA; UAS, upstream activating sequence.

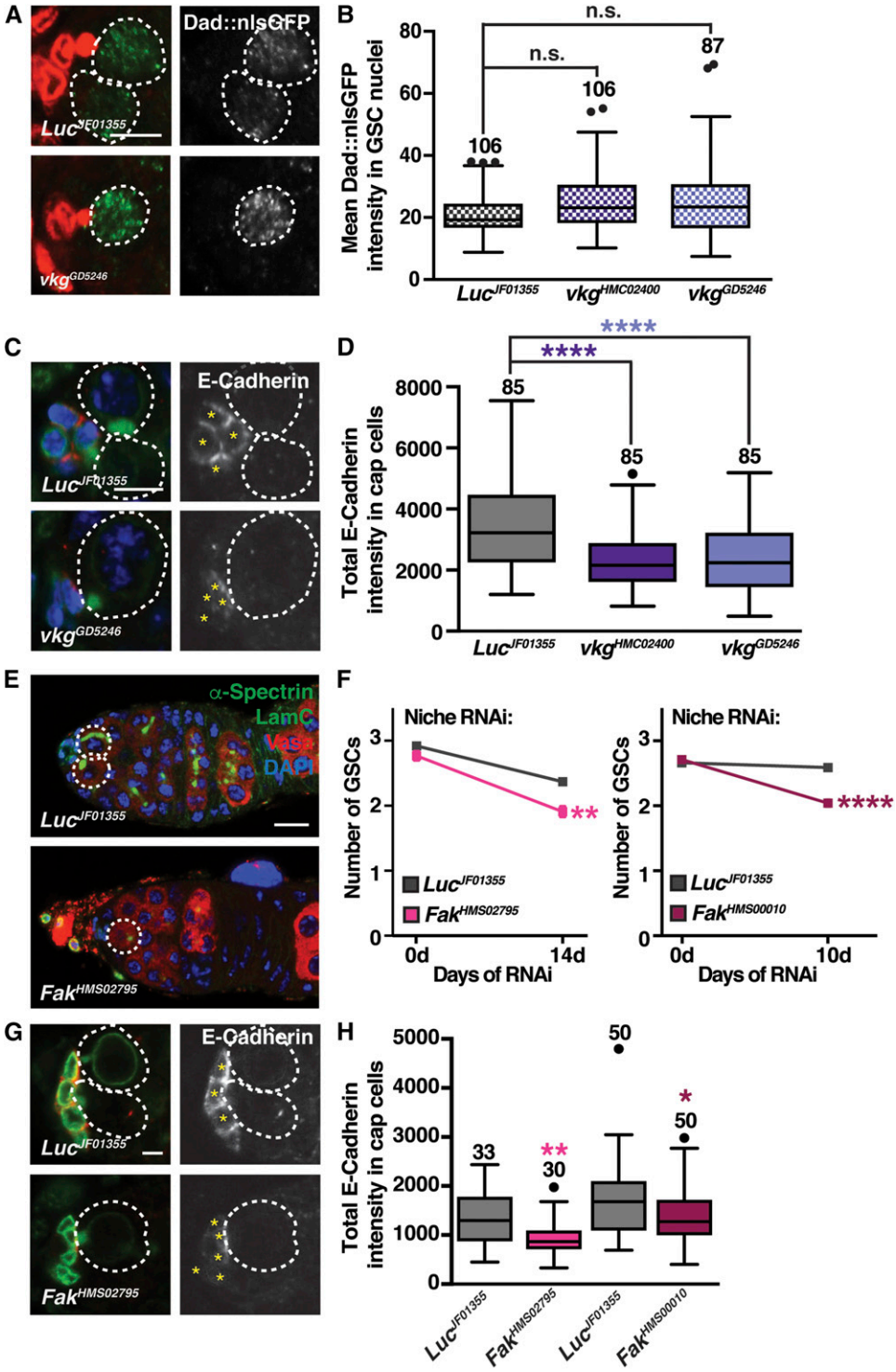

Figure 3 Adipocyte-derived collagen IV positively regulates E-cadherin levels at the GSC-niche interface through FAK. (A) Germaria from females at 10 days of adipocyte-specific *Luc* control or *vkg*^{GD5246} RNAi. GFP (green), Dad::nlsGFP; LamC (red), cap cell nuclear lamina; α-Spectrin (red), fusome. Dad::nls shown in grayscale in panels on the right. GSC nuclei are outlined. Bar, 5 μm. (B) Box-and-whisker plot of mean Dad::nlsGFP intensity for experiment in (A). (C) Germaria from females described in (A). E-cadherin (red); LamC (green), cap cell nuclear lamina; α-Spectrin (green), fusome; DAPI (blue), nuclei. E-Cadherin shown in grayscale in panels on the right and asterisks indicate cap cells. Bar, 5 μm. (D) Box-and-whisker plot of mean E-cadherin intensity for experiment in (C). Sample sizes in (B and D) are included above boxes. **** $P < 0.0001$, Mann–Whitney *U*-test. (E) Germaria from females at 14 days of knockdown of *Luc* or *Fak* in the adult niche showing Vasa (germ cells, red), α-spectrin (fusome, green), LamC (nuclear lamina, green), and DAPI (DNA, blue). Bar, 10 μm. (F) Average number of GSCs per germarium at 0, 10, and 14 days of *bab1*^{ts}-mediated induction of RNAi against *Fak* or *Luc* (mean ± SEM; ** $P < 0.01$ and **** $P < 0.0001$, two-way ANOVA with interaction). (G) Germaria at 10 days of adipocyte-specific *Luc* or *Fak* RNAi labeled for E-cadherin (red), LamC (nuclear lamina, green), and α-spectrin (fusome, green). E-cadherin shown in grayscale in panels on the right and asterisks indicate cap cells. Bar, 2.5 μm. (H) Box-and-whisker plot of mean E-cadherin intensity. Sample sizes are included above. **** $P < 0.0001$, Mann–Whitney *U*-test. The number of germaria analyzed is shown above each box. See also Figure S4. FAK, focal adhesion kinase; GSC, germline stem cell; n.s., not significant; RNAi, RNA interference.

upstream of collagen IV production/secretion in adipocytes and whether the influence of adipocyte-derived collagen IV on GSC maintenance is responsive to physiological factors such as diet, disease, or aging. Future studies should also address how collagen IV is transported from adult adipocytes, traverses the muscle sheath that encases the ovary, and then becomes incorporated into the established basement membrane of the GSC niche. Further, many additional key players that are secreted from adipocytes in response to physiological changes to regulate GSC number are as yet unidentified (Armstrong *et al.* 2014; Matsuoka *et al.* 2017). Although we are beginning to gain a better understanding of fat-to-ovary communication, much future work will be required to address the intricate mechanisms and the myriad

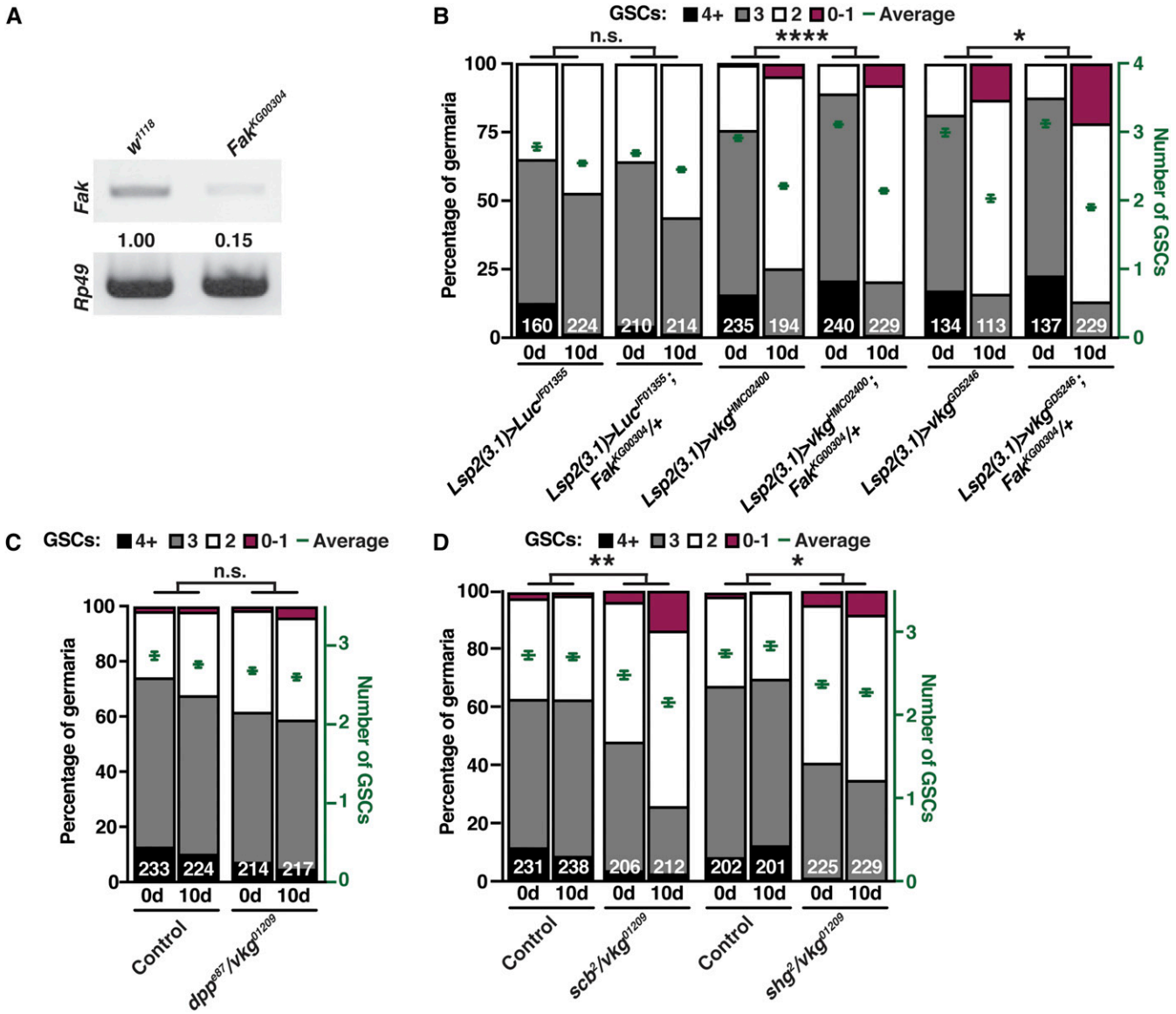

Figure 4 FAK interacts genetically with adipocyte collagen IV to regulate GSC numbers. (A) RT-PCR of *Fak* in w^{1118} or $Fak^{KG00304}$ homozygous females showing that the $Fak^{KG00304}$ hypomorphic allele has reduced levels of *Fak* mRNA expression. *Rp49* is used as a control. Normalized band intensities are indicated. (B) Frequencies of germaria containing zero-or-one, two, three, or four-or-more GSCs at 1 and 10 days of adipocyte-specific RNAi against *Luc* (control) or *vkg* RNAi in females carrying one copy of $Fak^{KG000304}$ compared to their balancer sibling controls without $Fak^{KG000304}$. The average number of GSCs per germarium is plotted in green. (C and D) Frequencies of germaria containing zero-or-one, two, three, or four-or-more GSCs in newly eclosed (0d) and 10-day-old (10d) double heterozygous dpp^{e87} +/+ vkg^{01209}, vkg^{01209} +/+ scb^{2}, or vkg^{01209} +/+ shg^{2} females compared to their balancer sibling (single heterozygous) controls are shown on the left *y*-axis. The right *y*-axis shows the average number of GSCs per germarium. The number of germaria analyzed is shown inside bars. Mean ± SEM. * $P < 0.05$, ** $P < 0.01$, and **** $P < 0.0001$, two-way ANOVA with interaction. FAK, focal adhesion kinase; GSC, germline stem cell; n.s., difference in slopes not statistically significant; RNAi, RNA interference.

of players mediating the interorgan communication that influences adult stem cell behavior and tissue homeostasis.

Acknowledgments

The data and analyses reported in this paper are described in the main figures and supplemental materials. We thank the Developmental Studies Hybridoma Bank for antibodies; the Bloomington Stock Center [National Institutes of Health (NIH) grant P40 OD-018537), Henrich Jasper, and William Chia for *Drosophila* stocks; and Tianlu Ma for critical reading of the manuscript. This work was supported by NIH grant R01 GM-069875 (D.D.-B.). L.N.W. was supported by NIH grants T32 CA-009110 and F32 GM-119199. The authors declare no conflicts of interest.

Author contributions: L.N.W. and D.D.-B. designed experiments, analyzed and interpreted data, and wrote the manuscript. L.N.W. performed all experiments.

Literature Cited

Ables, E. T., and D. Drummond-Barbosa, 2010 The steroid hormone ecdysone functions with intrinsic chromatin remodeling factors to control female germline stem cells in Drosophila. Cell Stem Cell 7: 581–592. https://doi.org/10.1016/j.stem.2010.10.001

Ables, E. T., and D. Drummond-Barbosa, 2013 Cyclin E controls Drosophila female germline stem cell maintenance independently of its role in proliferation by modulating responsiveness to niche signals. Development 140: 530–540. https://doi.org/10.1242/dev.088583

Ables, E. T., K. M. Laws, and D. Drummond-Barbosa, 2012 Control of adult stem cells in vivo by a dynamic physiological environment: diet-dependent systemic factors in Drosophila and beyond. Wiley Interdiscip. Rev. Dev. Biol. 1: 657–674. https://doi.org/10.1002/wdev.48

Ables, E. T., K. E. Bois, C. A. Garcia, and D. Drummond-Barbosa, 2015 Ecdysone response gene E78 controls ovarian germline stem cell niche formation and follicle survival in Drosophila. Dev. Biol. 400: 33–42. https://doi.org/10.1016/j.ydbio.2015.01.013

Ables, E. T., G. H. Hwang, D. S. Finger, T. D. Hinnant, and D. Drummond-Barbosa, 2016 A genetic mosaic screen reveals ecdysone-responsive genes regulating Drosophila oogenesis. G3 (Bethesda) 6: 2629–2642. https://doi.org/10.1534/g3.116.028951

Armstrong, A. R., K. M. Laws, and D. Drummond-Barbosa, 2014 Adipocyte amino acid sensing controls adult germline stem cell number via the amino acid response pathway and independently of target of rapamycin signaling in Drosophila. Development 141: 4479–4488. https://doi.org/10.1242/dev.116467

Arrese, E. L., A. D. Howard, R. T. Patel, O. J. Rimoldi, and J. L. Soulages, 2010 Mobilization of lipid stores in Manduca sexta: cDNA cloning and developmental expression of fat body triglyceride lipase, TGL. Insect Biochem. Mol. Biol. 40: 91–99. https://doi.org/10.1016/j.ibmb.2009.12.008

Asha, H., I. Nagy, G. Kovacs, D. Stetson, I. Ando *et al.*, 2003 Analysis of Ras-induced overproliferation in Drosophila hemocytes. Genetics 163: 203–215.

Ayyaz, A., H. Li, and H. Jasper, 2015 Hemocytes control stem cell activity in the Drosophila intestine. Nat. Cell Biol. 17: 736–748. https://doi.org/10.1038/ncb3174

Bonnans, C., J. Chou, and Z. Werb, 2014 Remodelling the extracellular matrix in development and disease. Nat. Rev. Mol. Cell Biol. 15: 786–801. https://doi.org/10.1038/nrm3904

Brizzi, M. F., G. Tarone, and P. Defilippi, 2012 Extracellular matrix, integrins, and growth factors as tailors of the stem cell niche. Curr. Opin. Cell Biol. 24: 645–651. https://doi.org/10.1016/j.ceb.2012.07.001

Cabrera, G. R., D. Godt, P. Y. Fang, J. L. Couderc, and F. A. Laski, 2002 Expression pattern of Gal4 enhancer trap insertions into the bric a brac locus generated by P element replacement. Genesis 34: 62–65. https://doi.org/10.1002/gene.10115

Canel, M., A. Serrels, M. C. Frame, and V. G. Brunton, 2013 E-cadherin-integrin crosstalk in cancer invasion and metastasis. J. Cell Sci. 126: 393–401. https://doi.org/10.1242/jcs.100115

de Cuevas, M., and A. C. Spradling, 1998 Morphogenesis of the Drosophila fusome and its implications for oocyte specification. Development 125: 2781–2789.

Dodson, G. S., D. J. Guarnieri, and M. A. Simon, 1998 Src64 is required for ovarian ring canal morphogenesis during Drosophila oogenesis. Development 125: 2883–2892.

Espinosa Neira, R., and E. P. Salazar, 2012 Native type IV collagen induces an epithelial to mesenchymal transition-like process in mammary epithelial cells MCF10A. Int. J. Biochem. Cell Biol. 44: 2194–2203. https://doi.org/10.1016/j.biocel.2012.08.018

Frantz, C., K. M. Stewart, and V. M. Weaver, 2010 The extracellular matrix at a glance. J. Cell Sci. 123: 4195–4200. https://doi.org/10.1242/jcs.023820

Fried, D., B. B. Bohm, K. Krause, and H. Burkhardt, 2012 ADAM15 protein amplifies focal adhesion kinase phosphorylation under genotoxic stress conditions. J. Biol. Chem. 287: 21214–21223. https://doi.org/10.1074/jbc.M112.347120

Haigo, S. L., and D. Bilder, 2011 Global tissue revolutions in a morphogenetic movement controlling elongation. Science 331: 1071–1074. https://doi.org/10.1126/science.1199424

Harburger, D. S., and D. A. Calderwood, 2009 Integrin signalling at a glance. J. Cell Sci. 122: 159–163. https://doi.org/10.1242/jcs.018093

Hsu, H. J., and D. Drummond-Barbosa, 2009 Insulin levels control female germline stem cell maintenance via the niche in Drosophila. Proc. Natl. Acad. Sci. USA 106: 1117–1121. https://doi.org/10.1073/pnas.0809144106

Hsu, H. J., and D. Drummond-Barbosa, 2011 Insulin signals control the competence of the Drosophila female germline stem cell niche to respond to Notch ligands. Dev. Biol. 350: 290–300. https://doi.org/10.1016/j.ydbio.2010.11.032

Hsu, H. J., L. LaFever, and D. Drummond-Barbosa, 2008 Diet controls normal and tumorous germline stem cells via insulin-dependent and -independent mechanisms in Drosophila. Dev. Biol. 313: 700–712. https://doi.org/10.1016/j.ydbio.2007.11.006

LaFever, L., and D. Drummond-Barbosa, 2005 Direct control of germline stem cell division and cyst growth by neural insulin in Drosophila. Science 309: 1071–1073. https://doi.org/10.1126/science.1111410

LaFever, L., A. Feoktistov, H. J. Hsu, and D. Drummond-Barbosa, 2010 Specific roles of Target of rapamycin in the control of stem cells and their progeny in the Drosophila ovary. Development 137: 2117–2126. https://doi.org/10.1242/dev.050351

Langer, C. C., R. K. Ejsmont, C. Schonbauer, F. Schnorrer, and P. Tomancak, 2010 In vivo RNAi rescue in Drosophila melanogaster with genomic transgenes from Drosophila pseudoobscura. PLoS One 5: e8928. https://doi.org/10.1371/journal.pone.0008928

Laws, K. M., and D. Drummond-Barbosa, 2015 Genetic mosaic analysis of stem cell lineages in the Drosophila ovary. Methods Mol. Biol. 1328: 57–72. https://doi.org/10.1007/978-1-4939-2851-4_4

Laws, K. M., and D. Drummond-Barbosa, 2016 AMP-activated protein kinase has diet-dependent and -independent roles in Drosophila oogenesis. Dev. Biol. 420: 90–99. https://doi.org/10.1016/j.ydbio.2016.10.006

Laws, K. M., and D. Drummond-Barbosa, 2017 Control of germline stem cell lineages by diet and physiology. Results Probl. Cell Differ. 59: 67–99. https://doi.org/10.1007/978-3-319-44820-6_3

Laws, K. M., L. L. Sampson, and D. Drummond-Barbosa, 2015 Insulin-independent role of adiponectin receptor signaling in Drosophila germline stem cell maintenance. Dev. Biol. 399: 226–236. https://doi.org/10.1016/j.ydbio.2014.12.033

Lee, J. Y., J. Y. Chen, J. L. Shaw, and K. T. Chang, 2016 Maintenance of stem cell niche integrity by a novel activator of integrin signaling. PLoS Genet. 12: e1006043. https://doi.org/10.1371/journal.pgen.1006043

Legate, K. R., S. A. Wickstrom, and R. Fassler, 2009 Genetic and cell biological analysis of integrin outside-in signaling. Genes Dev. 23: 397–418. https://doi.org/10.1101/gad.1758709

Mao, M., M. V. Alavi, C. Labelle-Dumais, and D. B. Gould, 2015 Type IV collagens and basement membrane diseases: cell biology and pathogenic mechanisms. Curr. Top. Membr. 76: 61–116. https://doi.org/10.1016/bs.ctm.2015.09.002

Matsubayashi, Y., A. Louani, A. Dragu, B. J. Sanchez-Sanchez, E. Serna-Morales *et al.*, 2017 A moving source of matrix components is essential for de novo basement membrane formation. Curr. Biol. 27: 3526–3534.e4. https://doi.org/10.1016/j.cub.2017.10.001

Matsuoka, S., A. R. Armstrong, L. L. Sampson, K. M. Laws, and D. Drummond-Barbosa, 2017 Adipocyte metabolic pathways regulated by diet control the female germline stem cell lineage in Drosophila melanogaster. Genetics 206: 953–971. https://doi.org/10.1534/genetics.117.201921

McGuire, S. E., P. T. Le, A. J. Osborn, K. Matsumoto, and R. L. Davis, 2003 Spatiotemporal rescue of memory dysfunction in Drosophila. Science 302: 1765–1768. https://doi.org/10.1126/science.1089035

Miles, A. J., A. P. N. Skubitz, L. T. Furcht, and G. B. Fields, 1994 Promotion of cell adhesion by sing-stranded and triple-helical peptide models of basement membrane collagen a1(IV) 531–543. J. Biol. Chem. 269: 30939–30945.

Mui, K. L., C. S. Chen, and R. K. Assoian, 2016 The mechanical regulation of integrin-cadherin crosstalk organizes cells, signaling and forces. J. Cell Sci. 129: 1093–1100. https://doi.org/10.1242/jcs.183699

Neely, G. G., K. Kuba, A. Cammarato, K. Isobe, S. Amann *et al.*, 2010 A global in vivo Drosophila RNAi screen identifies NOT3 as a conserved regulator of heart function. Cell 141: 142–153. https://doi.org/10.1016/j.cell.2010.02.023

Ni, J. Q., R. Zhou, B. Czech, L. P. Liu, L. Holderbaum *et al.*, 2011 A genome-scale shRNA resource for transgenic RNAi in Drosophila. Nat. Methods 8: 405–407. https://doi.org/10.1038/nmeth.1592

Pastor-Pareja, J. C., and T. Xu, 2011 Shaping cells and organs in Drosophila by opposing roles of fat body-secreted collagen IV and perlecan. Dev. Cell 21: 245–256. https://doi.org/10.1016/j.devcel.2011.06.026

Rodriguez, A., Z. Zhou, M. L. Tang, S. Meller, J. Chen *et al.*, 1996 Identification of immune system and response genes, and novel mutations causing melanotic tumor formation in Drosophila melanogaster. Genetics 143: 929–940.

Rosen, E. D., and B. M. Spiegelman, 2014 What we talk about when we talk about fat. Cell 156: 20–44. https://doi.org/10.1016/j.cell.2013.12.012

Song, X., and T. Xie, 2002 DE-cadherin-mediated cell adhesion is essential for maintaining somatic stem cells in the Drosophila ovary. Proc. Natl. Acad. Sci. USA 99: 14813–14818. https://doi.org/10.1073/pnas.232389399

Spradling, A. C., D. Stern, A. Beaton, E. J. Rhem, T. Laverty *et al.*, 1999 The Berkeley Drosophila genome project gene disruption project: single P-element insertions mutating 25% of vital Drosophila genes. Genetics 153: 135–177.

Stark, K. A., G. H. Yee, C. E. Roote, E. L. Williams, S. Zusman *et al.*, 1997 A novel alpha integrin subunit associates with betaPS and functions in tissue morphogenesis and movement during Drosophila development. Development 124: 4583–4594.

Tepass, U., and V. Hartenstein, 1994 Epithelium formation in the Drosophila midgut depends on the interaction of endoderm and mesoderm. Development 120: 579–590.

Tsai, P. I., H. H. Kao, C. Grabbe, Y. T. Lee, A. Ghose *et al.*, 2008 Fak56 functions downstream of integrin alphaPS3betanu and suppresses MAPK activation in neuromuscular junction growth. Neural Dev. 3: 26. https://doi.org/10.1186/1749-8104-3-26

Tseng, C. Y., S. H. Kao, C. L. Wan, Y. Cho, S. Y. Tung *et al.*, 2014 Notch signaling mediates the age-associated decrease in adhesion of germline stem cells to the niche. PLoS Genet. 10: e1004888 (erratum: PLoS Genet. 11: e1005766). https://doi.org/10.1371/journal.pgen.1004888

Van De Bor, V., G. Zimniak, L. Papone, D. Cerezo, M. Malbouyres *et al.*, 2015 Companion blood cells control ovarian stem cell niche microenvironment and homeostasis. Cell Rep. 13: 546–560. https://doi.org/10.1016/j.celrep.2015.09.008

Wang, H., V. Radjendirane, K. K. Wary, and S. Chakrabarty, 2004 Transforming growth factor beta regulates cell-cell adhesion through extracellular matrix remodeling and activation of focal adhesion kinase in human colon carcinoma Moser cells. Oncogene 23: 5558–5561. https://doi.org/10.1038/sj.onc.1207701

Wang, X., R. E. Harris, L. J. Bayston, and H. L. Ashe, 2008 Type IV collagens regulate BMP signalling in Drosophila. Nature 455: 72–77. https://doi.org/10.1038/nature07214

Wharton, K., R. P. Ray, and W. M. Gelbart, 1993 An activity gradient of decapentaplegic is necessary for the specification of dorsal pattern elements in the Drosophila embryo. Development 117: 807–822.

Xie, T., and A. C. Spradling, 1998 decapentaplegic is essential for the maintenance and division of germline stem cells in the Drosophila ovary. Cell 94: 251–260. https://doi.org/10.1016/S0092-8674(00)81424-5

Yano, H., Y. Mazaki, K. Kurokawa, S. K. Hanks, M. Matsuda *et al.*, 2004 Roles played by a subset of integrin signaling molecules in cadherin-based cell-cell adhesion. J. Cell Biol. 166: 283–295. https://doi.org/10.1083/jcb.200312013

Zabidi, M. A., and A. Stark, 2016 Regulatory enhancer-core-promoter communication via transcription factors and cofactors. Trends Genet. 32: 801–814. https://doi.org/10.1016/j.tig.2016.10.003

Communicating editor: M. Wolfner